Origibnal Article

Marked biochemical difference in amyloid proportion between intra- and extraocular tissues in a liver-transplanted patient with hereditary ATTR amyloidosis

Tsuneaki Yoshinaga[1], Masahide Yazaki[1,2], Fuyuki Kametani[3], Yoshiki Sekijima[1,2], Yasuhiro Iesato[4], Teruyoshi Miyahara[4], Ayako Tsuchiya-Suzuki[1], Kenji Sano[5], Keiichi Higuchi[2,6], Shu-ichi Ikeda[1]

[1]Department of Medicine (Neurology and Rheumatology), [4]Department of Ophthalmology, and [5]Department of Laboratory Medicine, Shinshu University School of Medicine, Matsumoto, Japan

[2]Department of Biological Sciences for Intractable Neurological Diseases, Institute for Biomedical Sciences, Shinshu University, Matsumoto, Japan

[3]Department of Dementia and Higher Brain Function, Tokyo Metropolitan Institute of Medical Science, Tokyo, Japan

[6]Department of Aging Biology, Institute of Pathogenesis and Disease Prevention, Shinshu University Graduate School of Medicine, Mastumoto, Japan

Running title: Proportion in ocular amyloid of ATTR-FAP

Correspondence: Masahide Yazaki, MD

Department of Biological Sciences for Intractable Neurological Diseases,

Institute for Biomedical Sciences, Shinshu University, Matsumoto 390-8621, Japan

Tel: +81-263-37-2673 Fax: +81-263-37-3427 E-mail: mayazaki@shinshu-u.ac.jp

Abstract

To elucidate the detailed pathomechanism of ocular amyloid formation in a liver-transplanted patient with hereditary ATTR amyloidosis, we investigated detailed biochemical features of ocular amyloid. The patient was a 49-year-old woman with V30M transthyretin (TTR) variant (p.TTRV50M), who underwent ophthalmectomy due to corneal rupture 10 years after liver transplantation (LT). The amyloid was selectively isolated from several portions in intra- and extraocular tissues using a laser microdissection (LMD) system and analyzed by liquid chromatography-tandem mass spectrometry to determine the composition percentage of wild-type and variant TTR in the isolated amyloid. Biochemical analysis revealed that the amyloid consisted mainly of variant TTR in intraocular tissues with a percentage > 80%. On the other hand, in the extraocular muscles, wild-type TTR was the main component of the amyloid with a percentage of ~70%. Our data indicate that intraocular amyloid formation strongly depends on locally synthesized variant TTR and the contribution of wild-type TTR to amyloid formation is quite limited.

Keywords: hereditary ATTR amyloidosis, ocular amyloidosis, transthyretin, liver transplantation, laser microdissection

Introduction

Hereditary ATTR amyloidosis, traditionally called familial amyloid polyneuropathy (ATTR-FAP) is an inherited systemic amyloidosis characterized by peripheral somatic and autonomic neuropathy with the involvement of many visceral organs [1]. The causative amyloid precursor proteins are single amino acid substitution variants of transthyretin (TTR). As the majority of TTR is synthesized in the liver, liver transplantation (LT) abolishes the hepatic source of variant TTR and is one of the most promising therapies for hereditary ATTR amyloidosis patients [2]. However, a number of studies have suggested that the involvement of several organs, especially the heart, eyes, and central nervous system, can deteriorate or newly occur even after LT [3-8]. Our previous studies demonstrated that postoperative progression of amyloid cardiomyopathy results from ongoing deposition of wild-type TTR-derived amyloid [3,4]. On the other hand, as postoperative ophthalmological manifestations, vitreous opacities and secondary glaucoma are well known to occur in hereditary ATTR amyloidosis patients after LT [5,6,9]. With regard to the biochemical features of ocular amyloid fibril proteins after LT, only vitreous amyloid has been investigated using vitrectomy samples [6,10,11]. As TTR is also produced in the retinal pigment epithelium (RPE) and ciliary pigment epithelium [12,13], it has been postulated that the progression of postoperative vitreous amyloid may result from local synthesis of variant TTR in the eye [6,10,11]. However, the precise pathomechanism of postoperative ocular amyloidosis, in particular the role of wild-type TTR in ocular amyloid formation and the pathogenesis in intraocular portions other than the vitreous body, is not fully understood, because of the lack of biochemical data for ocular amyloid fibrils except vitreous amyloid and of comparative data between intra- and extraocular tissue amyloid in the

same transplanted patients. In addition, it has been nearly impossible to extract amyloid fibrils separately from various portions of a small organ, such as the eyeball, with conventional amyloid extraction methods involving tissue homogenization [14].

In this study, in addition to the histopathological features, we report the detailed biochemical characteristics of intra- and extraocular tissue amyloid extracted from an enucleated whole eyeball from a hereditary ATTR amyloidosis patient 10 years posttransplantation. The amyloid was separately isolated from various parts of intra- and extraocular tissues using a laser microdissection (LMD) system and were biochemically investigated by liquid-chromatography tandem mass spectrometry (LC-MS/MS)-based proteomics analysis.

Material and Methods

Patient

The patient was a 49-year-old woman with heterozygous V30M TTR variant (ATTRV30M, p.V50M), who had a family history of hereditary ATTR amyloidosis. At age 37, she began to have blurred vision because of vitreous opacities in both eyes. She also noted orthostatic dizziness and numbness in the legs due to sensory and autonomic neuropathy. At age 39, she underwent LT and her visual acuity was 1.0/0.6 with normal intraocular pressure (IOP) (10/10 mmHg, normal 10-20 mmHg). However, visual acuity progressively worsened to 0.06/0.03p4 by age of 41 due to deterioration of vitreous opacities and cataract (**Fig. 1AB**). At age 41, vitrectomy and cataract surgery were performed on the left eye with implantation of an intraocular lens. Bilateral glaucoma gradually occurred with high IOP (max. 52/54 mmHg) and she underwent bilateral trabeculectomy at age 46. However, the IOP in the left eye could not be controlled, and

she also underwent glaucoma implant surgery into the left eye 3 months later. She suffered with intermittent severe nausea and vomiting, and her physical condition progressively worsened. She became severely emaciated and almost bedridden. At age 49 (10 years after LT), she was admitted to our hospital for repeated syncope due to hypotension and left hemiplegia. Ophthalmological examination demonstrated corneal ulcer in the left eye, and then the left eye suddenly ruptured at the corneal ulcer. Thus, the left eye was enucleated (**Fig. 1C**).

Histopathological evaluation of the eyeball

The removed left eye was fixed in 10% formalin and paraffin-embedded tissue sections were prepared. Amyloid deposits were identified with Congo red staining. Evaluation of the grade of amyloid deposition was carried out as follows according to the previous report [15]: +, slight and localized deposition; ++, moderate deposition; +++, severe and diffuse deposition.

Immunohistochemical analysis was also performed using anti-TTR antiserum [16] to confirm that the deposited amyloid was derived from TTR (**Fig. 1D**).

Amyloid extraction and preparation for biochemical investigation using an LMD system and LC-MS/MS

Using an LMD system (LMD7000; Leica Microsystems Inc., Tokyo, Japan), the deposited amyloid was separately isolated from intraocular tissues, including the iris, vessels in the ciliary body, retina, retinal vessels, and vessels in the sclera (**Fig. 1C,2**). Amyloid was also isolated from remnant vitreous body (**Fig. 1C,2**). On the other hand, as the extraocular tissues, the amyloid was extracted from vessels in extraocular

muscles attached to the enucleated eyeball and optic nerve sheath (**Fig. 1C,3**). In addition, duodenal mucosae biopsied at age 45 were also investigated (**Fig. 3**). Sections of paraffin-embedded samples 6 μm thick were placed on slide glasses with special foil for LMD (Leica Microsystems Inc., Tokyo, Japan) and stained with Congo red. Microdissected tissues were solubilized in 50 μl of 10 mM Tris/1 mM EDTA/0.002% Zwittergent 3-16 (Calbiochem, San Diego, CA) buffer with heating at 98°C for 90 minutes and sonication for 60 minutes, and were digested with trypsin overnight at 37°C [17].

Evaluation of the biochemical amyloid proportion of wild-type and variant TTR

To determine the percentage of wild-type (V30) and variant TTR (M30) in the deposited amyloid, the relative quantification of tryptic peptides (TTR 22-34 with V30 or M30) was performed by LC-MS/MS (Nano LC DiNa; KYA Technologies Co., Tokyo Japan and QExactive or Velos Pro; Thermo Fisher Scientific Inc., Waltham, MA) as reported previously [18,19]. The chromatograms were filtered with mass ranges, m/z 683.50-685.0, m/z 699.50-701.00, and m/z 707.50-709.00. These ranges correspond to TTR 22-34 wild-type (GSPAINVA**V**HVFR, m/z 683.88), variant peptide (GSPAINVA**M**HVFR, m/z 699.87), and variant peptide oxidized at Met-30 (GSPAINVA**M(ox)**HVFR, m/z 707.87), respectively. The investigation was repeated twice and the mean composition ratio was calculated.

This study was performed with the approval of the Institutional Review Board of Shinshu University and with written informed consent from the patient.

Results

Histopathological findings of the eyeball

Microscopic examination demonstrated that the choroid and retina were completely detached from the sclera with some hematoma (**Fig. 1C**). The corneal ulcer was present and some intraocular amyloid-rich material containing vitreous body, pieces of iris, and detached retina leaked out from the perforated cornea (**Fig. 1C, Supplemental Fig.**). Mild infiltration of inflammatory cells was also seen **(Supplemental Fig.**).

TTR-related amyloid deposits were widely seen in intra- and extraocular tissues (**Fig. 1C,D, Table 1**). In particular, severe amyloid deposits were present on the surface and inside the iris and ciliary body (**Fig. 2, Supplemental Fig.**). Amyloid deposits were also observed on the vessels walls and on the inner limiting membrane of the retina. No amyloid deposition was observed in the neuroepithelial layer of the retina (**Fig. 2**). Amyloid deposition was found in the sclera and in the choroid, but the amount of deposits was mild and mainly localized to vessel walls (**Fig. 2**). Moderate amyloid deposition was observed in the trabecular meshwork around Schlemm's canal (**Supplemental Fig.**). No amyloid was detected in the cornea (**Supplemental Fig.**).

On the other hand, in extraocular tissues, there was no amyloid deposition in the optic nerve fibers but marked amyloid deposits were observed in the optic nerve sheath (**Fig. 1C**,**3A,B**). In the peri-optic nerve tissues, amyloid deposits were seen on the vascular walls and in the endoneurium of the short ciliary nerve containing sensory nerve fibers and autonomic nerve fibers from the ciliary ganglion (**Fig. 1C, Supplemental Fig.**). In extraocular muscles and duodenal mucosa, moderate to severe amyloid deposition was also detected mainly on the interstitial vessel walls (extraocular muscles) (**Fig. 3C,D**) and on the lamina muscularis mucosae (duodenum) (**Fig. 3E,F**).

Percentage of wild-type and variant TTR in the deposited amyloid fibril protein

The percentages of wild-type and variant TTR in the deposited amyloid fibrils are shown in **Table 1** and representative data of LC-MS/MS analysis of microdissected amyloid protein are presented in **Fig. 4**. In intraocular tissues, including the iris, ciliary body, remnant vitreous body, choroid, and retina, the percentage of variant TTR was uniformly high (84% - 98%). The percentage of variant TTR was also extremely high in retinal vessel amyloid (94%). On the other hand, in extraocular muscles, the contribution of wild-type TTR to amyloid composition was more remarkable (71%), and was almost the same as in duodenal mucosal amyloid (69%). In the vessels of the sclera and optic nerve sheath, the ratio of variant TTR was high (61% - 68%), but the contribution of variant TTR was not remarkable compared to other intraocular tissues.

Discussion

To date, there have been no detailed histopathological studies on postoperative ocular tissues in transplanted patients with hereditary ATTR amyloidosis. In the present patient, severe amyloid deposition was seen in the iris, the ciliary body, and the remnant vitreous body. While retinal amyloid angiopathy is a rare ocular manifestation in hereditary ATTRV30M amyloidosis patients [15,20], amyloid deposition was clearly found on the retinal vessels, as described previously in a hereditary amyloidosis patient with ATTRY114C, a unique type of TTR variant causing severe oculoleptomenigial amyloidosis [20]. This pathological evidence suggests that the occurrence of retinal angiopathy and its clinical importance will also increase with posttransplantation time even in patients with hereditary ATTRV30M amyloidosis.

With regard to the investigation of amyloid fibril proteins, our data showed that there was a marked difference in the biochemical component between intra- and extraocular tissue amyloid, although both were histopathologically the same on Congo red staining. Of particular interest is that the amyloid was composed mainly of variant TTR with almost the same percentages (over 80%) in all intraocular tissues except for the sclera. The contribution of wild-type TTR to intraocular amyloid formation is markedly limited. These results were the same as those in a previous biochemical study of vitreous amyloid in a transplanted patient with hereditary ATTR amyloidosis (88% variant TTR) [6]. These observations indicate that intraocular amyloid is formed with quite high dependence on variant TTR.

On the other hand, the amyloid was composed predominantly of wild-type TTR in extraocular tissues. Although the retina was completely detached from the sclera in our patient, the retina is inherently adjacent to extraocular muscles at a distance of only 2 or 3 mm, sandwiching the sclera (**Fig. 1C**). Despite such close location, there were marked differences in the biochemical features of amyloid fibrils between the vessels in the retina and in the extraocular muscles, suggesting that amyloid is constructed by a different mechanism between intra- and extraocular tissues. In the postoperative amyloid formation on the vessels of extraocular muscles, the contribution of circulating wild-type TTR may be remarkable. As plasma TTR cannot diffuse through the blood–ocular barriers [21], it is likely that the amyloid fibrils were uniformly formed mainly with locally synthesized variant TTR in intraocular tissues of the present patient. In this study, the outcomes of the amyloid proportion were the same between the sclera and the optic nerve sheath, which were almost intermediate between the values of the intraocular and extraocular tissues. The optic nerve sheath is directly connected to the

sclera. Thus, the pathomechanism of amyloid formation may be similar between the sclera and the optic nerve sheath under the influence of locally synthesized variant TTR and wild-type TTR, locally synthesized or produced from the liver.

However, it is still unclear why the contribution of wild-type TTR to amyloid formation in intraocular tissues is limited, although wild-type TTR is also produced equally with variant TTR in the eye [22]. In the present patient, the proportion of variant TTR in amyloid fibrils on the vessels of choroid was also high. The choroidal capillaries, which are different from the retinal vessels with tight junctions, are fenestrated vessels that act as the major blood suppliers for the neuroepithelial layer of the retina [21], and it should therefore be possible for circulating hepatic wild-type TTR to be involved in amyloid formation on vascular walls of the choroid. However, wild-type TTR was not actually included at significant levels in the amyloid formation. Even in non-transplanted FAP, the proportion of wild-type TTR in the vitreous amyloid fibrils is low (less than 20%) [23,24], similar to the data in our transplanted FAP patient. Thus, these biochemical data may show that wild-type TTR becomes much less amyloidogenic inside the eye, compared to that in other visceral organs. In our recent study in a hereditary ATTRV30M amyloidosis patient that died 18 years after LT, the amyloid in the central nervous system also consisted mainly of variant TTR (over 90%) [8]. Hence, the pathophysiology of amyloidogenesis differs markedly between intra- and extraocular or cerebral tissues, and ocular or cerebral amyloid formation seems to depend quite strongly on locally synthesized variant TTR, regardless of LT.

Finally, as a recent clinical study indicated that ocular manifestations in transplanted patients with hereditary ATTR amyloidosis were not influenced by LT [25], our biochemical data also clearly show that progression of ocular manifestations in

hereditary ATTR amyloidosis patients cannot be prevented by LT. Thus, we emphasize that establishment of other therapeutic options to halt the local synthesis of variant TTR in the eye is necessary to maintain the quality of life in hereditary ATTR amyloidosis patient, who can survive much longer than before by LT or other therapeutic options such as the TTR-stabilizers.

Acknowledgement

This study was supported by grants from the Amyloid Research Committee, Intractable Disease Division, Ministry of Health, Labour and Welfare in Japan, Amyloid Research, a Grant-in-Aid for Scientific Research, Ministry of Education, Culture, Sports, Science and Technology in Japan (26670152 to KH, MY), and a grant from the Hokuto Foundation for Bioscience (TY, MY).

Declaration of Interest

The authors have no dualities of interest to declare.

References

1. Ikeda S, Nakazato M, Ando Y, Sobue G. Familial transthyretin-type amyloid polyneuropathy in Japan: clinical and genetic heterogeneity. Neurology 2002;58:1001-1007.
2. Holmgren G, Steen L, Ekstedt J, Groth CG, Ericzon BG, Eriksson S, et al. Biochemical effect of liver transplantation in two Swedish patients with familial amyloidotic polyneuropathy (FAP me30). Clin Genet 1991;40:242-246.
3. Yazaki M, Tokuda T**,** Nakamura A, Higashikata T, Koyama J, Higuchi K, et al**.** Cardiac amyloid in patients with familial amyloid polyneuropathy consists of abundant wild-type transthyretin. Biochem Biophys Res Commun 2000;274:702-706.
4. Yazaki M, Mitsuhashi S, Tokuda T, Kametani F, Takei Y, Koyama J, et al. Progressive wild-type transthyretin deposition after liver transplantation preferentially occurs onto myocardium in FAP patients. Am J Transplant 2007;7:235-2342.
5. Ando Y, Ando E, Tanaka Y, Yamashita T, Tashima K, Suga M, et al. De novo amyloid synthesis in ocular tissue in familial amyloidotic polyneuropathy after liver transplantation. Transplantation 1996;62:1037-1038.
6. Ando E, Ando Y, Haraoka K. Ocular amyloid involvement after liver transplantation for polyneuropathy. Ann Int Med 2001;135:931-932.
7. Salvi F, Pastorelli F, Plasmati R, Morelli C, Rapezzi C, Bianchi A, et al. Brain microbleeds 12 years after orthotopic liver transplantation in Val30Met amyloidosis. J Stroke Cerebrovasc Dis. 2015;24:e149-151.
8. Sekijima Y, Yazaki M, Oguchi K, Ezawa N, Yoshinaga T, Yamada M, et al. Cerebral amyloid angiopathy in posttransplant patients with hereditary ATTR amyloidosis. Neurology 2016;87:773-781.

9. Hara R, Kawaji T, Ando E, Ohya Y, Ando Y, Tanihara H, et al. Impact of liver transplantation on transthyretin-related ocular amyloidosis in Japanese patients. Arch Opthalmol 2010;128:206-210.
10. Munar-Qués M, Salvá-Ladaria L, Mulet-Perera P, Solé M, López-Andreu FR, Saraiva MJ, et al. Vitreous amyloidosis after liver transplantation in patients with familial amyloid polyneuropathy: ocular synthesis of mutant transthyretin. Amyloid 2000;7:266-269.
11. Liepnieks JJ, Phan ADT, Wise RJ, Hrisomalos FN, Benson MD. Biochemical characterization of vitreous amyloid formed after liver transplantaion. Amyloid 2016;23:136-137
12. Cavallaro T, Martone RL, Dwork AJ, Schon EA, Herbert J, et al. The retinal pigment epithelium is the unique site of transthyretin synthesis in the rat eye. Invest Ophthalmol Vis Sci 1990;31:497-501.
13. Kawaji T, Ando Y, Nakamura M, Yamamoto K, Ando E, Takano A, et al. Transthyretin synthesis in ciliary pigment epithelium. Exp Eye Res 2005;81:306-312.
14. Pras M, Schubert M, Zucker-Franklin D, Rimon A, Franklin EC. The characterization of soluble amyloid prepared in water. J Clin Invest 1968;47:924-933
15. Haraoka K, Ando Y, Ando E, Sandgren O, Hirata A, Nakamura M, et al. Amyloid deposition in ocular tissues of patients with familial amyloidostic polyneuropathy (FAP). Amyloid 2002;9:183-189.
16. Gustavsson A, Engström U, Westermark P. Mechanisms of transthyretin amyloidogenesis. Antigenic mapping of transthyretin purified from plasma and

amyloid fibrils and within in situ tissue localizations. Am J Pathol 1994;144:1301-1311.

17. Sethi S, Theis JD, Vrana JA, Fervenza FC, Sethi A, Qian Q, et al. Laser microdissection and proteomic analysis of amyloidosis, cryoglobulinemic GN, fibrillary GN, and immunotoctoid glomerulopathy. Clin J AM Soc Nephrol 2013;8:915-921.
18. Kametani F, Haga S. Accumulation of carboxy-terminal fragments of APP increases phosphodiesterase 8B. Neurobiol Aging 2015;36:634-637.
19. Yoshinaga T, Yazaki M, Sekijima Y, Kametani F, Miyashita K, Hachiya N, et al. The pathological and biochemical identification of possible seed-lesions of transmitted transthyretin amyloidosis after domino liver transplantation. J Path Clin Res 2016;2:72-79
20. Kawaji T, Ando Y, Nakamura M, Yamashita T, Wakita M, Ando E, et al. Ocular amyloid angiopathy associated with familial amyloidotic polyneuropathy caused by amyloidogenic transthyretin Y114C. Opthalmology 2005;112:2212-2218.
21. Beirão JM, Moreira LV, Lacerda PC, Vitorino RP, Beirão IB, Torres PA, et al. Inability of mutant transthyretin V30M to cross the blood-eye barrier. Transplantation 2012;94:e54-e56.
22. Haraoka K, Ando Y, Ando E, Sun X, Nakamura M, Terazaki H, et al. Presence of variant transthyretin in aqueous humor of a patient with familial amyloidotic polyneuropathy after liver transplantation. Amyloid 2002;9:247-251.
23. Ando Y, Ando E, Ohlsson PI, Olofsson A, Sandgren O, Suhr O, et al. Analysis of transthyretin amyloid fibrils from vitreous samples in familial amyloidotic polyneuropathy (Val30Met). Amyloid 1999;6:119-123.

24. Liepnieks JJ, Wilson DL, Benson MD. Biochemical characterization of vitreous and cardiac amyloid in Ile84Ser transthyretin amyloidosis. Amyloid 2006;13:170-177.
25. Beirão JM, Malheiro J, Lemos C, Matos E, Beirão I, Pinho-Costa P, et al. Impact of liver transplantation on the natural history of oculopathy in Portugese patients with transthyretin (V30M) amyloidosis. Amyloid 2015;22:31-35.

Figure Legends

Fig. 1: Posttransplantation ophthalmological findings of the left eye (A,B), Congored-stained axial view of the enucleated eye (C), and immunohistochemistry using anti-TTR antiserum (D).

The photo of the optic fundus of the left eye at 2 years after LT (A) shows severe vitreous opacities and the findings significantly deteriorated at 9 years after LT, where the papilla could not be identified (B). Congo red-stained view of the enucleated eye demonstrates the presence of amyloid deposits almost entirely in the ocular tissues (C). The arrow indicates the portion of corneal rupture and arrowheads indicate hematomas. Retina and choroid are completely detached from the sclera. EOM: Extraocular muscles. Opt. N: Optic nerve. PON: Peri-optic nerve tissues. VB: Remnant vitreous body. Immunohistochemical study using anti-TTR antibody [16] clearly confirmed that the deposited amyloid was associated with TTR (D).

Fig. 2: Congo red-stained histological findings of intraocular tissues.

A,B: Iris border. C: Remnant vitreous body. D,E: Retina. F,G: Choroid. H,I: Sclera. B,E,G,I: Views under polarized light. Abundant amyloid deposition was seen on the iris (A,B), vitreous (C), and retina (inner limiting membrane and vessels) (D,E). Amyloid deposits were localized on vascular walls in choroid (F,G) and in sclera (H,I). No amyloid deposition was observed in the neuroepithelial layer of the retina. The detached retina was folded making a double layer so that both inner limiting membranes were inside (D,E). IM: Inner limiting membrane. NEL: Neuroepithelial layer. RPE: Retinal pigment epithelium.

Fig. 3: Congo red-stained histological findings of extraocular tissues.

A,B: Optic nerve (Opt. N). C,D: Extraocular muscles. E,F: Duodenal mucosa.

B,D,F: Views under polarized light.

No amyloid deposition was observed in the optic nerve fibers but marked amyloid deposits were seen in the dura mater of the optic nerve sheath (A,B). In extraocular muscles (C,D) and duodenal mucosa (E,F), moderate to severe amyloid deposition was also found mainly on the interstitial vessel walls of extraocular muscles and on the lamina muscularis mucosae of the duodenum.

Fig. 4. Representative data of relative quantification of TTR 22-34 tryptic peptide in LC-MS/MS analysis of amyloid fibrils isolated from the iris (A), retinal vessels (B), optic nerve sheath (C), and vessels in extraocular muscles (D).

The biochemical composition percentages of wild-type vs. variant TTR in amyloid were 2%:98% (A, iris), 6%:94% (B, retinal vessels), 32%:68% (C, optic nerve sheath), and 71%:29% (D, vessels in extraocular muscles), respectively. Arrows denote the peaks derived from TTR 22-34 peptides contaninig V30, M30, or oxidized M30 (Mox).

Supplemental Fig. Other portions of Congo red-stained intra- and extraocular tissues

A,B: Corneal ulcer with perforation. C,D: Ciliary body and trabecular meshwork around Schlemm's canal. E,F: Peri-optic nerve tissues. B,D,F: Views under polarized light.

A,B: The corneal ulcer was present with mild infiltration inflammatory cells but amyloid deposition was not seen in the cornea. Some intraocular amyloid-rich material containing vitreous body, pieces of iris, and detached retina leaked out from the

perforated cornea. C,D: In the trabecular meshwork (T) around Schlemm's canal (S), moderate amyloid deposition was observed . AC: Anterior chamber. E,F: In peri-optic nerve tissues (PON), amyloid deposits were seen on the vascular walls and in the endoneurium of short ciliary nerve (white arrows).

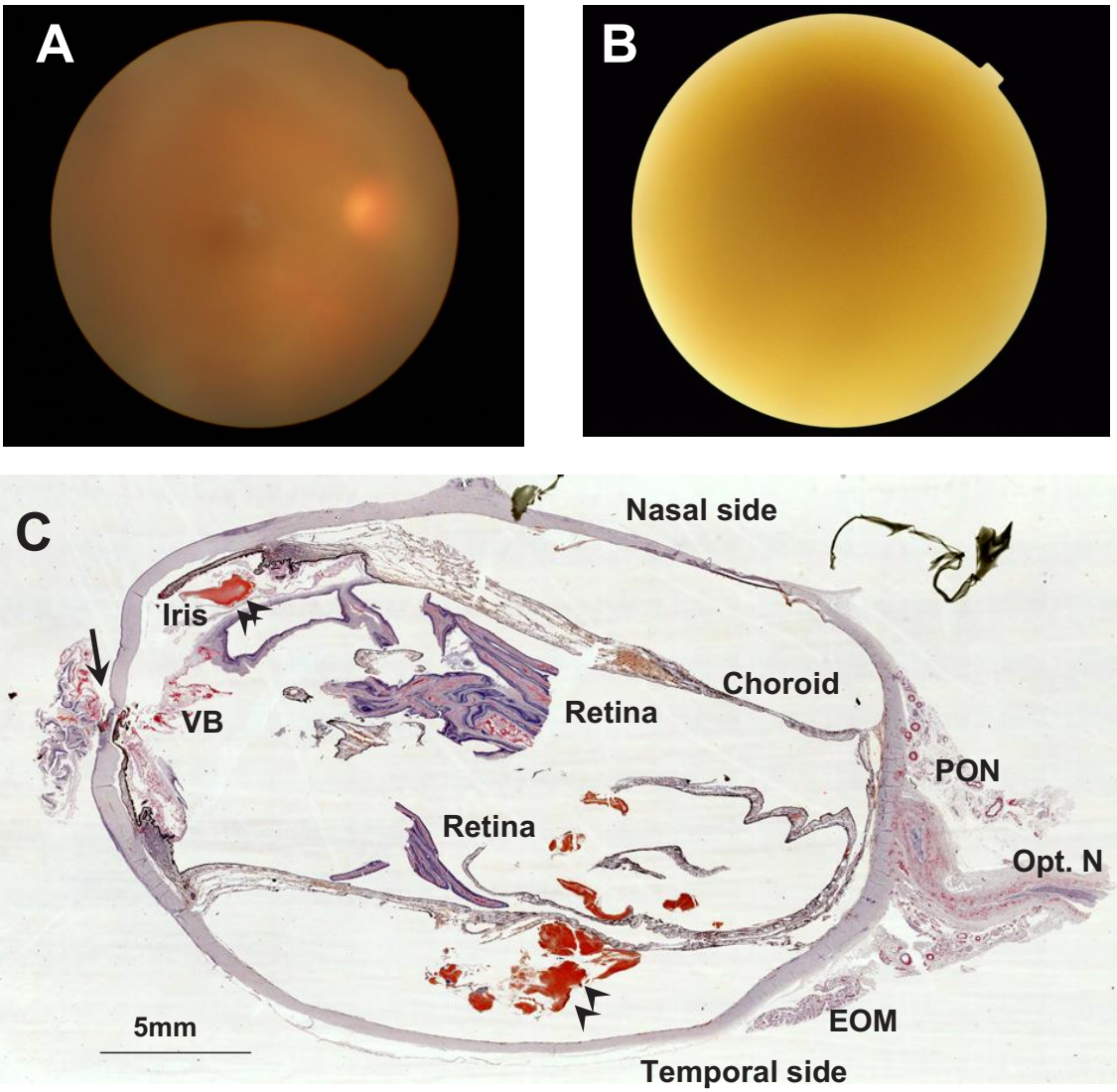
A
B
C
Nasal side
Iris
VB
Choroid
Retina
PON
Retina
Opt. N
5mm
EOM
Temporal side
D
5mm

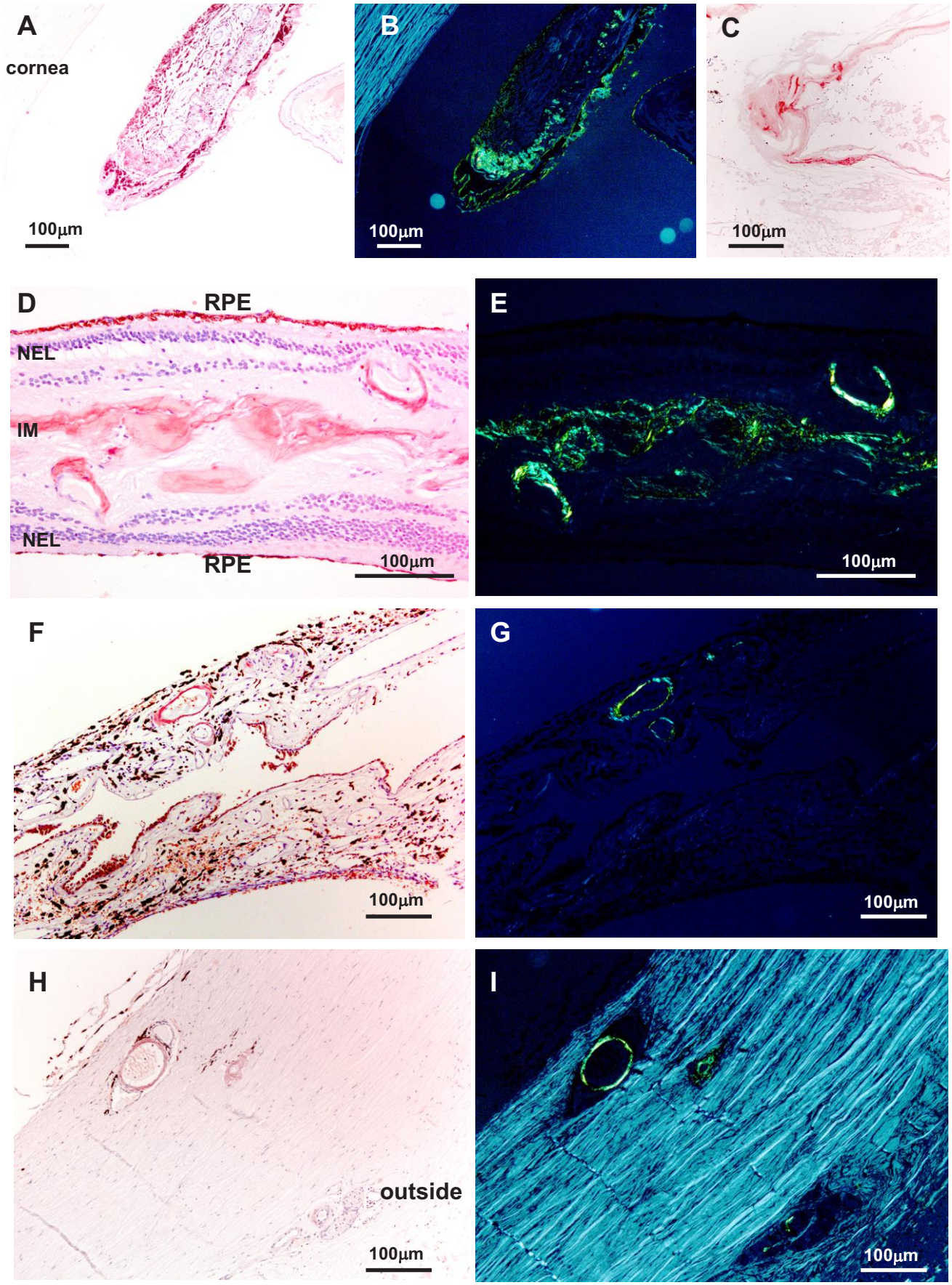
A
cornea
100μm
B
100μm
C
100μm
D
RPE
NEL
IM
NEL
RPE
100μm
E
100μm
F
100μm
G
100μm
H
outside
100μm
I
100μm

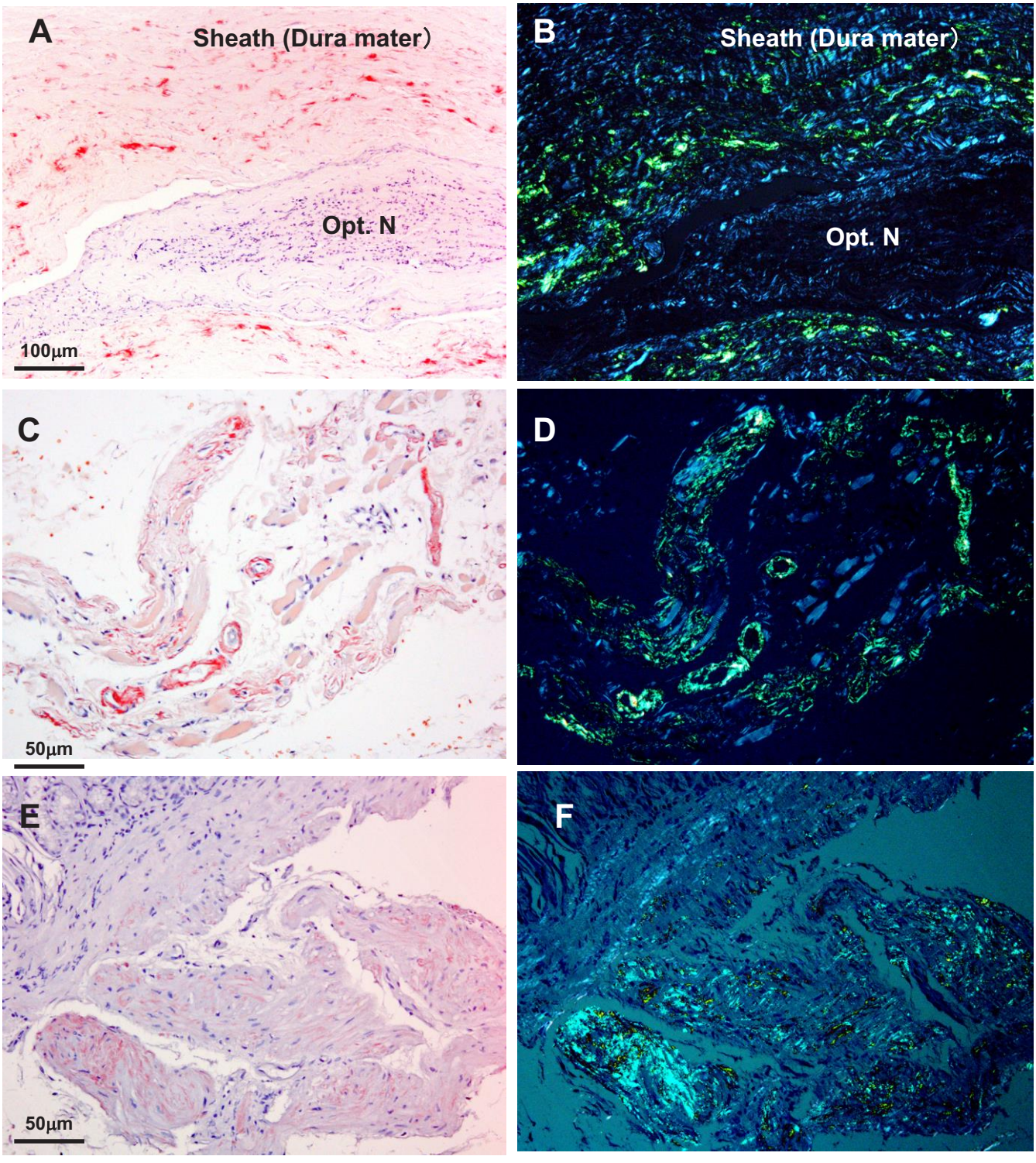
A
Sheath (Dura mater)
Opt. N
100μm
B
Sheath (Dura mater)
Opt. N
C
50μm
D
E
50μm
F

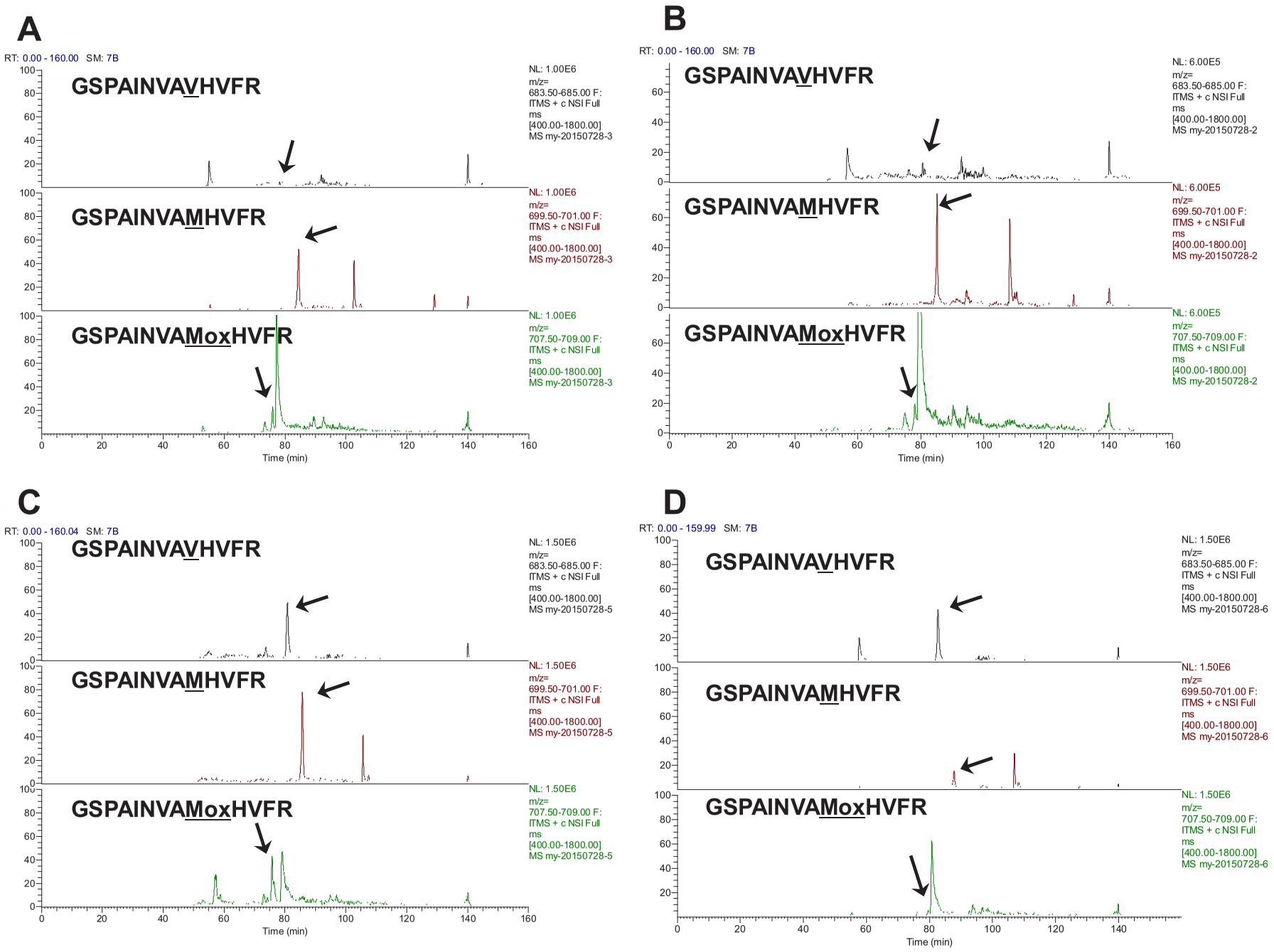
A
RT: 0.00 - 160.00 SM: 7B
GSPAINVAVHVFR
NL: 1.00E6
m/z=
683.50-685.00 F:
ITMS + c NSI Full
ms
[400.00-1800.00]
MS my-20150728-3
GSPAINVAMHVFR
NL: 1.00E6
m/z=
699.50-701.00 F:
ITMS + c NSI Full
ms
[400.00-1800.00]
MS my-20150728-3
GSPAINVAMoxHVFR
NL: 1.00E6
m/z=
707.50-709.00 F:
ITMS + c NSI Full
ms
[400.00-1800.00]
MS my-20150728-3
Time (min)
B
RT: 0.00 - 160.00 SM: 7B
GSPAINVAVHVFR
NL: 6.00E5
m/z=
683.50-685.00 F:
ITMS + c NSI Full
ms
[400.00-1800.00]
MS my-20150728-2
GSPAINVAMHVFR
NL: 6.00E5
m/z=
699.50-701.00 F:
ITMS + c NSI Full
ms
[400.00-1800.00]
MS my-20150728-2
GSPAINVAMoxHVFR
NL: 6.00E5
m/z=
707.50-709.00 F:
ITMS + c NSI Full
ms
[400.00-1800.00]
MS my-20150728-2
Time (min)
C
RT: 0.00 - 160.04 SM: 7B
GSPAINVAVHVFR
NL: 1.50E6
m/z=
683.50-685.00 F:
ITMS + c NSI Full
ms
[400.00-1800.00]
MS my-20150728-5
GSPAINVAMHVFR
NL: 1.50E6
m/z=
699.50-701.00 F:
ITMS + c NSI Full
ms
[400.00-1800.00]
MS my-20150728-5
GSPAINVAMoxHVFR
NL: 1.50E6
m/z=
707.50-709.00 F:
ITMS + c NSI Full
ms
[400.00-1800.00]
MS my-20150728-5
Time (min)
D
RT: 0.00 - 159.99 SM: 7B
GSPAINVAVHVFR
NL: 1.50E6
m/z=
683.50-685.00 F:
ITMS + c NSI Full
ms
[400.00-1800.00]
MS my-20150728-6
GSPAINVAMHVFR
NL: 1.50E6
m/z=
699.50-701.00 F:
ITMS + c NSI Full
ms
[400.00-1800.00]
MS my-20150728-6
GSPAINVAMoxHVFR
NL: 1.50E6
m/z=
707.50-709.00 F:
ITMS + c NSI Full
ms
[400.00-1800.00]
MS my-20150728-6
Time (min)

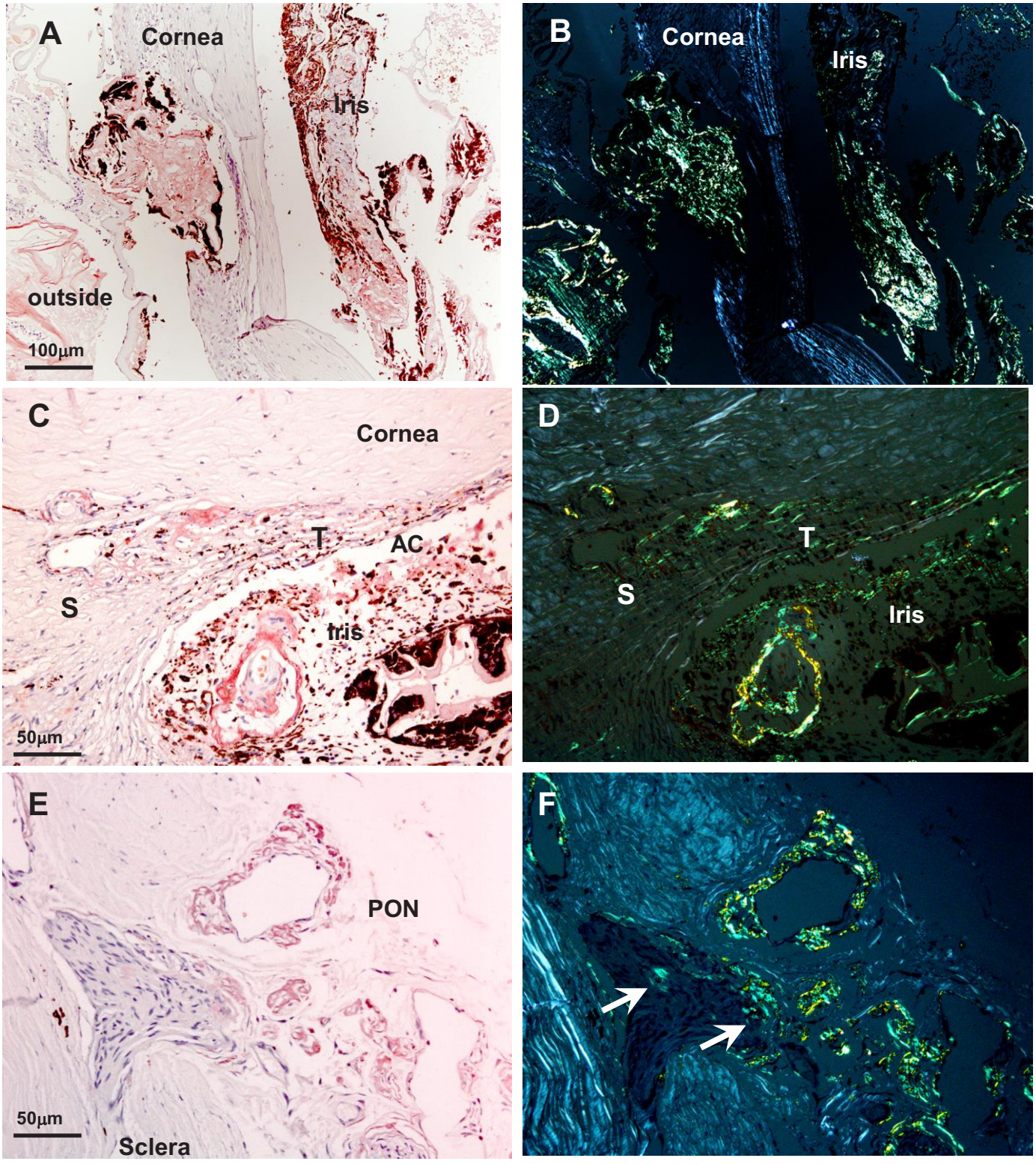
A
Cornea
Iris
outside
100μm
B
Cornea
Iris
C
Cornea
T
AC
S
Iris
50μm
D
T
S
Iris
E
PON
50μm
Sclera
F

Table 1. The severity of amyloid deposits and biochemical proportion of amyloid fibrils

	Tissues	Amyloid deposits	Mean TTR composition percentage (%)	
			Wild type	Variant
Intra-ocular tissues	Cornea	-	NE	NE
	Iris	+++	2	98
	Ciliary body	+++	10	90
	Trabecular meshwork	++	NE	NE
	Remnant vitreous body	+++	3	97
	Retina	+++	3	97
	Retinal vessels	+++	6	94
	Choroid	+	16	84
	Sclera	+	39	61
Extra-ocular tissues	Optic nerve fibers	-	NE	NE
	Optic nerve sheath	+++	32	68
	Peri-optic nerve tissues	+++	NE	NE
	Extraocular muscles	++	71	29
	Duodenum	++	69	31

Grade of amount of amyloid deposits [14]: -: none, +: slight and localized, ++: moderate, +++: severe
NE: not examined